Nuclear Instruments and Methods in Physics Research B 539 (2023) 141–147

Contents lists available at ScienceDirect

Nuclear Inst. and Methods in Physics Research, B

journal homepage: www.elsevier.com/locate/nimb

Total electron yield (TEY) detection mode Cr K-edge XANES spectroscopy as a direct method to probe the composition of the surface of darkened chrome yellow ($PbCr_{1-x}S_xO_4$) and potassium chromate paints

Letizia Monico [a,b,c,*], Francesco d'Acapito [d], Marine Cotte [e,f], Koen Janssens [c,g], Aldo Romani [a,b], Giulia Ricci [b], Costanza Miliani [h], Laura Cartechini [a]

[a] CNR-SCITEC, c/o Department of Chemistry, Biology and Biotechnology, University of Perugia, Via Elce di Sotto 8, 06123 Perugia, Italy
[b] Centre of Excellence SMAArt and Department of Chemistry, Biology and Biotechnology, University of Perugia, Via Elce di Sotto 8, 06123 Perugia, Italy
[c] AXIS Research Group, NANOlab Centre of Excellence, Department of Physics, University of Antwerp, Groenenborgerlaan 171, 2020 Antwerp, Belgium
[d] CNR-IOM-OGG, c/o ESRF LISA CRG, Avenue des Martyrs 71, 38000 Grenoble, France
[e] ESRF, Avenue des Martyrs 71, 38000 Grenoble, France
[f] LAMS, CNRS UMR 8220, Sorbonne Université, UPMC Univ Paris 06, Place Jussieu 4, 75005 Paris, France
[g] Rijksmuseum, Conservation & Restoration—Scientific Research, Hobbemastraat 22, 1071 ZC Amsterdam, The Netherlands
[h] CNR-ISPC, Via Cardinale Guglielmo Sanfelice 8, 80134 Napoli, Italy

ARTICLE INFO

Keywords:
Synchrotron radiation
X-rays
XANES
Lead chromate
Cultural heritage
Chromium
Degradation
Art conservation

ABSTRACT

The darkening of chromate-pigments, including chrome yellows ($PbCr_{1-x}S_xO_4$), is a surface phenomenon affecting late 19th-early 20th c. paintings, such as those by Van Gogh. Exploring analytical strategies that contribute to a deep understanding of darkening is therefore significant for the long-term conservation of unique masterpieces.

Here, we examined the capabilities of Cr K-edge XANES spectroscopy collected at the same time in X-ray fluorescence yield (XFY) and total electron yield (TEY) detection modes to selectively study the surface composition of darkened oil paint mock-ups composed of chrome yellow ($PbCr_{0.2}S_{0.8}O_4$) or potassium chromate. By discussing advantages and drawbacks in using XFY/TEY modes in relation to XFY μ-XANES analysis from sectioned samples, we aim at assessing if TEY-XANES spectroscopy: (i) is a selective surface method to determine the abundance of different Cr-species from paint fragments; (ii) can contribute to optimize the analytical strategy by limiting time consuming sample preparation procedures; (iii) can decrease the probability of radiation damage.

1. Introduction

Darkening or fading of paints, often accompanied by loss of their stability due to chemical changes of the pigments and/or the binding medium, affect many cultural heritage objects, with serious risks for their preservation and management.

For a number of inorganic pigments, including Prussian blue ($MFe^{III}[Fe^{II}(CN)_6]\cdot\times H_2O$, with $M = K^+$, NH_4^+ or Na^+) [1,2], vermilion red (α-HgS) [3,4], orpiment (α-As_2S_3) [5–8], cadmium yellows ($Cd_{1-x}Zn_xS$) [9–14] and reds ($CdS_{1-x}Se_x$) [15], the color changes that are observed in paintings and other artefacts are the result of redox reactions. The process is a surface phenomenon, leading to the formation of amorphous and/or crystalline secondary products that usually produce layers of limited size within the paint stratigraphy; in most cases, the altered layer at the surface has a thickness below *ca.* 10 μm.

The past few decades have seen significant growth in the use of synchrotron radiation (SR)-based X-ray methods with micro-/nano-beams in the field of paintings conservation. Micro-X-ray absorption near edge structure (μ-XANES) spectroscopy in X-ray fluorescence yield (XFY) detection mode was often employed to perform non-destructive stratigraphic elemental speciation analysis of non-transparent amorphous or crystalline samples down to the (sub)micrometer scale length [16,17].

Nevertheless, sample preparation in the form of cross-section is generally demanding and time consuming, with characteristics that depend on the nature of the analyzed material and technical features of

* Corresponding author at: CNR-SCITEC, c/o Department of Chemistry, Biology and Biotechnology, University of Perugia, Via Elce di Sotto 8, 06123 Perugia, Italy.
E-mail address: letizia.monico@cnr.it (L. Monico).

https://doi.org/10.1016/j.nimb.2023.03.040
Received 30 November 2022; Received in revised form 20 January 2023; Accepted 28 March 2023
Available online 10 April 2023

the method of investigation (e.g., set-up geometry, energy of the incident beam…) [18]. In addition, sampling usually gives access to submicrometric areas of the artwork surface, with the consequence that, in some cases, the composition of the analyzed micro-samples might be not fully representative of the studied phenomena.

Thus, it becomes relevant to explore in-depth how SR-based X-ray methods may permit to obtain direct surface elemental speciation information from larger, non-transparent and layered fragments, while minimizing time consuming and lengthy sample preparation procedures.

In this context, total electron yield (TEY) detection mode has been proved to be a suitable alternative to indirect XAS measurements in XFY mode because of the shallowness of the electron escape depth (of the order of tens of nm) compared with X-ray fluorescence [19–22]. Its use, despite limited to few case studies in the field of heritage science, has been successfully exploited for performing elemental speciation investigations of different kind of objects, including lustre decoration of Italian Renaissance pottery [23], historical wooden buildings [24], degraded zinc yellow and copper resinate paints [25,26].

In the present study, we systematically explore the capabilities of Cr K-edge XANES spectroscopy collected at the same time in XFY and TEY detection modes to perform Cr speciation investigations of the surface of a set of darkened chromate-based yellow oil paints made up of either the light-sensitive sulfate-rich chrome yellow type ($PbCr_{0.2}S_{0.8}O_4$, hereafter denoted as $Cr_{0.2}Y$) or potassium chromate (K_2CrO_4). As the above-mentioned pigments, both class of compounds undergo darkening as a result of a reduction process of the original Cr^{VI} to Cr^{III}-compounds, with Cr^{V}-species arising from the interaction between the pigment and the oily medium [27–29]. This reaction has been identified as the cause of darkening in a number of paintings by Vincent van Gogh [30,31].

The technical advantages and drawbacks in using either XFY or TEY detection modes are presented and discussed in relation to XFY mode μ-XANES analysis from sectioned samples. This is done in order to assess if: (i) TEY-XANES spectroscopy with an unfocused beam may be employed as a selective method to determine the relative abundance of different Cr-species directly at the surface of degraded paint fragments; (ii) it can contribute to optimize analytical strategy by limiting time consuming sample preparation procedures; (iii) it may help to reduce the probability of radiation damage, considering the tendency of chromate-based compounds towards photo-reduction under the exposure to X-ray beams [32,33].

2. Materials and methods

2.1. Preparation of paint mock-ups and aging protocol

Paint mock-ups were prepared on polycarbonate slices by employing either mainly orthorhombic $PbCr_{0.2}S_{0.8}O_4$ (synthesized in our laboratory) or commercial orthorhombic K_2CrO_4 (Sigma-Aldrich) in mixture with cold-pressed linseed oil (Zecchi) in a 4:1 wt ratio.

Further information on the synthesis, crystalline structure, molecular properties and chemical reactivity of both compounds are reported in previous studies [27–29,34,35].

All paints were left to dry in the dark at temperatures of 25–35 °C and 35–45% relative humidity (RH) (i.e., measured indoor temperature and humidity level). As described earlier [27], as consequence of the higher solubility of K_2CrO_4 with respect to $Cr_{0.2}Y$ in the oily binder, K_2CrO_4 oil paint films naturally undergo darkening within a few days (i.e., before that the drying process has occurred), while $Cr_{0.2}Y$ paints do not behave the same. Thus, data from not altered paints were collected after *ca.* 1 month and after only *ca.* 10 h for $Cr_{0.2}Y$ paint (touch-dried system; hereinafter called "unaged") and for K_2CrO_4 sample (denoted "0 days"), respectively.

Since the well-known light-sensitivity of oil paints composed of sulfate-rich chrome yellow types [28,29], the accelerated artificial photochemical aging was performed only for $Cr_{0.2}Y$ mock-up. The treatment was carried out at ~20–35% RH (measured indoor humidity level) by means of a UVA-visible light ($\lambda > 300$ nm) emitted by a UV-filtered 300 W Cermax xenon lamp (see ref. [29] for the corresponding emission spectrum). The measured irradiance and temperature at the sample position were $\sim 5 \times 10^5$ μW/cm^2 and 25–30 °C, respectively. The paint was irradiated for 960 h to achieve a total radiant exposure value of $\sim 5 \times 10^7$ μW/cm^2·h). K_2CrO_4 paint was naturally aged in the dark, under environmental conditions of relative humidity (~30–40% RH) and temperature (25–30 °C) for 4 months, until a significant darkening of the paint surface was visible with the naked eye (for further details see ref. [27]).

2.2. XFY/TEY mode XANES spectroscopy at Cr K-edge

Cr K-edge XANES investigations of paint mock-ups were performed at the beamline BM08-LISA [36] and at the scanning X-ray microscope end station of beamline ID21 of the European Synchrotron Radiation Facility (ESRF, Grenoble, France) [37,38].

Measurements were carried out under 0.5 atm He atmosphere with a Si(3 1 1) crystal at BM08-LISA and under vacuum using a Si(2 2 0) fixed exit double-crystal monochromator at ID21.

At BM08-LISA, data were collected using an average beam size of $\sim 70 \times 100$ μm^2 (h × v) and a fluence rate of ~10^4 ph/(s·μm^2). An appropriate sample holder [39], equipped with a collecting anode polarized at ~20 V and placed at about 10 mm from the sample, allowed performing simultaneously XANES measurements in two different detection modes: (i) TEY and (ii) XFY. To guarantee an adequate conductivity of the sample during TEY analysis, a small fragment of each paint (~20–30 mm^2 size) was fixed with carbon adhesive tape on the sample holder. The He atmosphere was used as an electron amplifier as described in previous literature [40]. Spectra were recorded by scanning the primary energy of the incident beam across the Cr K-edge with the following steps (345 points; 3 s/pt): 5.8892–5.9692 keV, step: 10 eV; (ii) 5.9742–6.0496 keV, step: 0.25 eV; (iii) 6.0499–6.5375 keV, step: from 3 to 9 eV. The energy resolution of the monochromator was previously found to be coinciding with the theoretical values (see ref. [36]). In our case, considering the intrinsic resolution of the Si(3 1 1) crystal $\Delta E/E = 2.8 \times 10^{-5}$ [41], the resolution at the Cr K-edge is about 0.2 eV. A Cr metallic foil was used as a calibrant and a spectrum was collected at the same time as the sample to ensure the energy scale stability, which resulted to be better than 0.01 eV. For each sample, a total of 2–4 spectra were acquired.

At ID21, the incident beam was focused with a Kirkpatrick-Baez mirror system down to a spot size of $\sim 0.6 \times 0.3$ μm^2 (h × v) and, without beam attenuation, with a fluence rate of ~10^{10} ph/(s·μm^2). μ-XANES spectra in XFY mode were recorded from thin sections of the aged mock-ups (thickness of 10–15 μm) by scanning the primary energy of the incident beam across the Cr K-edge (5.95–6.087 keV) with increments of 0.2 eV (640 points; 0.1 s/pt). At this energy and under the employed experimental conditions the spectral resolution is 0.5 eV. For the calibration, the first inflection point of the first-order derivative Cr K-edge XANES spectrum of a Cr metallic foil was set at 5.9892 keV. For normalization purposes, a photodiode upstream the sample was constantly monitoring the beam intensity. μ-XRF mapping was performed *via* raster scanning of the samples with 40 ms/pixel dwell time and using a 80 mm^2 collimated active area silicon drift diode detector (Xflash 5100, Bruker). Cr oxidation state maps acquired from K_2CrO_4 mock-up were extracted by means of the PyMca software [42], after setting the energy of the incident X-ray beam at two energies: (i) at 5.993 keV, for promoting the excitation of Cr^{VI}-species, and (ii) at 6.090 keV for collecting XRF signals of all Cr-species. Details about the procedure employed to extract the Cr oxidation state maps are described elsewhere [43].

The ATHENA software package [44] was employed for the normalization and for the linear combination fitting (LCF) of the BM08-LISA and ID21 XANES spectra against a library of spectral profiles of Cr-

reference powders. This procedure allowed the relative abundance of Cr^{VI}-species (expressed as $\%[Cr^{VI}]/[Cr_{total}]$) and of reduced Cr-compounds (i.e., Cr^{V} and Cr^{III}) to be determined quantitatively. In XFY mode, spectra are usually affected by self-absorption effects. However, results obtained from the LCF to the ID21-XFY spectra by including in the model fit either XFY or transmission mode reference XANES spectra are comparable within an error of *ca.* 10%. In TEY mode, spectral profiles are not affected by self-absorption effects and data acquired in TEY mode and transmission are in general similar [45]. Consequently, all the LCF calculations were performed using reference spectra recorded in transmission mode for the two beamlines.

The X-ray penetration depth as a function of the angle of the incident beam at the Cr K-edge energy (*cf.* Fig. 5) was obtained using the JGIXA software package [46]. The sampling depth of the photoelectrons (predominantly originated by cascades of the Cr KLL Auger electrons at 4.8 keV [47]) was estimated by following the procedure earlier reported in the literature [21].

By following what we described in a previous study [32], a series of X-ray-induced damage tests at variable fluence conditions were performed on paint mock-ups both at BM08-LISA and ID21 to ensure that any Cr reduction process was not significantly impacting results.

3. Results

To explore the capabilities of Cr K-edge TEY-XANES spectroscopy in performing selective surface Cr speciation investigations, we started with the study of fragments of $Cr_{0.2}Y$ and K_2CrO_4 paint mock-ups at beamline BM08-LISA.

In line with previous studies [27–29,43], the photoaging treatment of $Cr_{0.2}Y$ and the natural aging of K_2CrO_4 promote a significant darkening of the paint surface (Figs. 1A–2A).

Cr K-edge XANES spectroscopy data collected at the same time in XFY and TEY detection modes from unaged-$Cr_{0.2}Y$ and 0 days-K_2CrO_4 paint mock-ups reveal that only Cr^{VI}-compounds are present (Figs. 1B–2B red lines; only the XFY spectra are reported as example). This is highlighted by the intense pre-edge peak at 5.993 keV, attributed to a dipole-forbidden transition from the Cr 1s orbital into orbitals with Cr 3d character (t_2 symmetry). Changes in the features of the post-edge absorption region reflect the different Cr local environments in the crystal structures of $Cr_{0.2}Y$ and K_2CrO_4 [43,48,49–51].

In both aged paints (Figs. 1B–2B, black and grey lines), the partial conversion of tetrahedral Cr^{VI} to octahedral Cr^{III}-compounds is pointed out by the decreasing of the pre-edge peak intensity (quantitatively proportional to the Cr^{VI} to total Cr content ratio) and by a shift of the absorption edge energy [43,48,50,51]. Nevertheless, the contribution of reduced Cr-species is higher in the spectrum recorded in TEY mode than XFY mode, as shown by a more significant decrease of the pre-edge peak intensity (see inset) and shift of the absorption edge towards lower energy along with a loss of structure of the post-absorption features. This result can be explained considering the lower sampling depth of TEY mode measurements with respect to XFY mode analysis, that, under the employed experimental conditions, allows the composition of the superficial brownish layer to be probed selectively.

To better correlate the TEY-XANES results obtained from the direct analysis of the aged paint surface with the stratigraphic distribution of different Cr-species at the submicrometric scale length, we carried out Cr K-edge μ-XANES spectroscopy investigations at beamline ID21 on thin sections obtained from the photoaged $Cr_{0.2}Y$ and the 4-months naturally aged K_2CrO_4 paint.

As illustrated in the microphotographs of Figs. 3A–4A, a brownish layer of about 5 μm and 20 μm thickness is clearly visible at the surface of $Cr_{0.2}Y$ and K_2CrO_4 paints, respectively.

The XFY mode μ-XANES spectra recorded from the uppermost darkened layer of both the aged $Cr_{0.2}Y$ and K_2CrO_4 thin sections (Figs. 3B–4B; black lines "top") show features very similar to the ones recorded in TEY modes directly at the altered surface of both paints

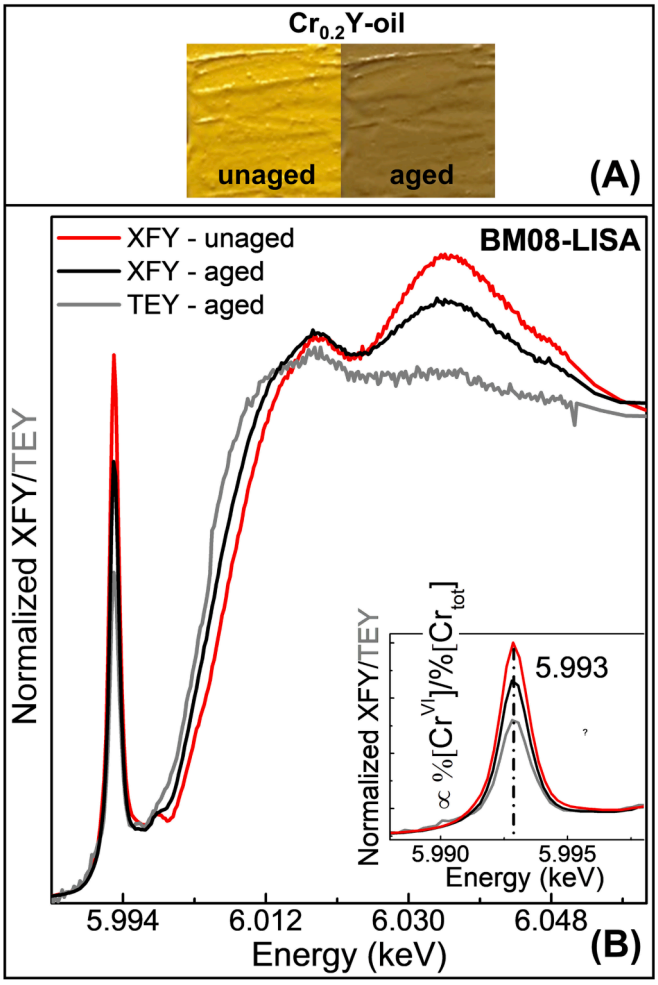

Fig. 1. Photographs of sulfate rich-chrome yellow type ($PbCr_{0.2}S_{0.8}O_4$) paint mock-ups before (left) and after artificial aging with UVA-visible light (right). (B) Cr K-edge XANES spectra collected from the surface of unaged/aged $Cr_{0.2}Y$ paints in XFY mode (red and black) and TEY mode (grey) at BM08-LISA.

(grey lines). In line with our previous studies [27], the results obtained by LCF of the XFY and TEY mode (μ-)XANES spectra highlight that the abundance of reduced Cr [likely a mixture of Cr^{III}-oxides, organo-Cr^{III} compounds and/or oxochromate(V)-complexes] is ~50% and ~75–80% within the uppermost darkened layer of $Cr_{0.2}Y$ and K_2CrO_4 paints, respectively. XFY mode μ-XANES profiles reveal that Cr^{VI}-species are instead dominant in the bulk yellow paint of both samples (black lines "bulk"). In addition, Cr oxidation state maps recorded from a region of interest of the aged K_2CrO_4 paint contribute to visualize more clearly the stratigraphic distribution of different Cr-species, showing that the brownish alteration layer is mainly composed of reduced Cr-compounds, while Cr^{VI}-species are homogeneously present as the main component of the yellow paint (Fig. 4C). Overall, the stratigraphic outcomes further support the hypothesis that the discrepancies observed between the XFY and TEY-XANES spectra recorded directly at the surface of the aged paints (Figs. 1B–2B) are related to the different sampling depth of the two techniques.

4. Discussion

In what follows, the results described in Section 3 will be employed to discuss and compare the technical features of TEY and XFY-XANES analysis from $Cr_{0.2}Y$ and K_2CrO_4 paint fragments (performed at BM08-LISA) and sectioned samples (carried out at ID21) with reference to penetration depth, probability of radiation damage, quality and

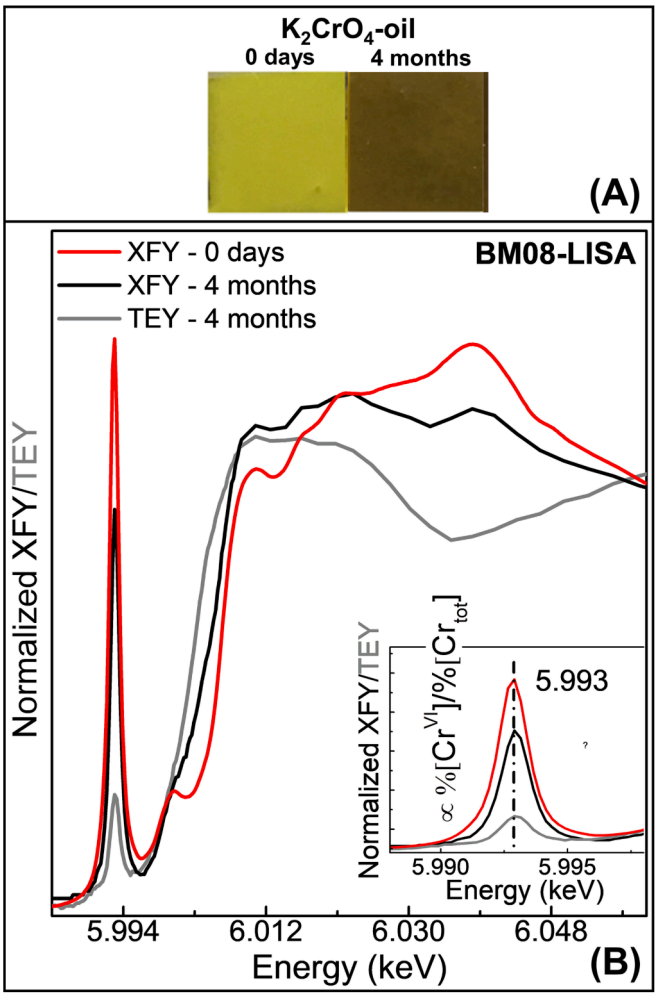

Fig. 2. (A) Photographs of K_2CrO_4 paint mock-ups collected immediately (0 days) and 4 months after preparation. (B) Cr K-edge XANES spectra recorded from the surface of 4-months naturally aged K_2CrO_4 paint in XFY mode (red and black) and TEY mode (grey) at BM08-LISA.

representativeness of acquired datasets and samples preparation.

As previously observed in different research fields, such as catalysis [52], superconducting materials [53], and optoelectronics technology [54], by carrying out comparative Cr K-edge XANES experiments with combined XFY/TEY detection mode we found that, TEY is a suitable surface-sensitive technique to provide selective Cr speciation information directly at the darkened paint surface (Figs. 1B–2B). At BM08-LISA, under the employed experimental conditions (incident and XFY detection angles from the surface: 70° and 20°, respectively), the X-ray penetration depth at the Cr K-edge (5.9892 keV) (Fig. 5) is higher/comparable with respect to the thickness of the superficial alteration layer, being of the order of ~5 μm and ~20 μm in $Cr_{0.2}Y$ and K_2CrO_4 paints, respectively (Figs. 3A–4A), whereas the layer sampled by the electrons is estimated to be of ~60 nm in $Cr_{0.2}Y$ and ~130 nm in K_2CrO_4 using a He-amplifier detector [21] and would be the double using a collecting anode in vacuum [20]. These calculations, along with the results obtained from thin sections at ID21 (Figs. 3 and 4), justify the higher relative abundance of Cr^{VI}-species observed in the XFY-XANES spectra with respect to the TEY-ones collected from the surface of paint fragments.

When measuring XANES in TEY mode at the surface of the sample, the beam does not need to be focused (conversely to the micro-analysis of cross-sections) and can indeed be laterally spread over tens or hundreds of micrometers. It follows that, under comparable conditions of

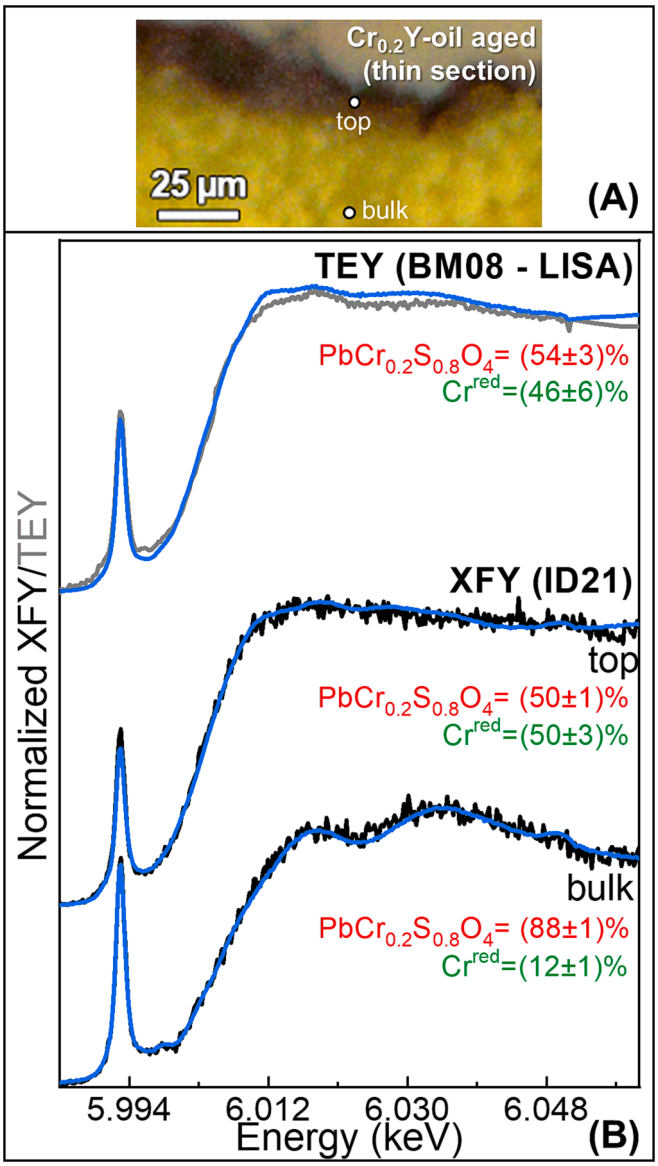

Fig. 3. (A) Microphotograph of a thin section obtained from the aged $Cr_{0.2}Y$ paint, showing the spots where data of (B) were recorded. (B) Result of the linear combination fit (cyan) of the XANES spectra of $PbCr_{0.2}S_{0.8}O_4$ and one/two Cr^{III}-references [namely: $Cr(OH)_3/Cr_2O_3$ and Cr^{III}-acetate/Cr^{III}-acetylacetonate] to the ones recorded from the surface of the aged $Cr_{0.2}Y$ paint in TEY mode at BM08-LISA (grey) and from the uppermost alteration layer (top) and the bulk paint (bulk) of the thin section in XFY mode at ID21 (black).

flux and energy, the probability of radiation damage is reduced. In that respect, fluences of ~10^6-10^7 ph/μm^2 were employed at BM08-LISA, that, based on our previous investigations [32], is of a ~10^4-10^5 factor below the threshold value for safe analysis of chrome yellow paints. Thus, in principle, further improvements in terms of both definition and signal to noise ratio of the acquired spectra might be possible, by selecting smaller energy step values and using longer dwell times per points.

TEY-XANES spectroscopy, as a surface-sensitive method for obtaining solid Cr speciation information directly from the study of the surface of fragments, brings also benefits in terms of samples preparation (much faster and less challenging with respect to the preparation of thin sections) and representativeness of the analyzed material, through access to larger portion of the degraded surface.

On the other hand, within the specific context of our experiment, TEY-XANES approach has a series of drawbacks, namely:

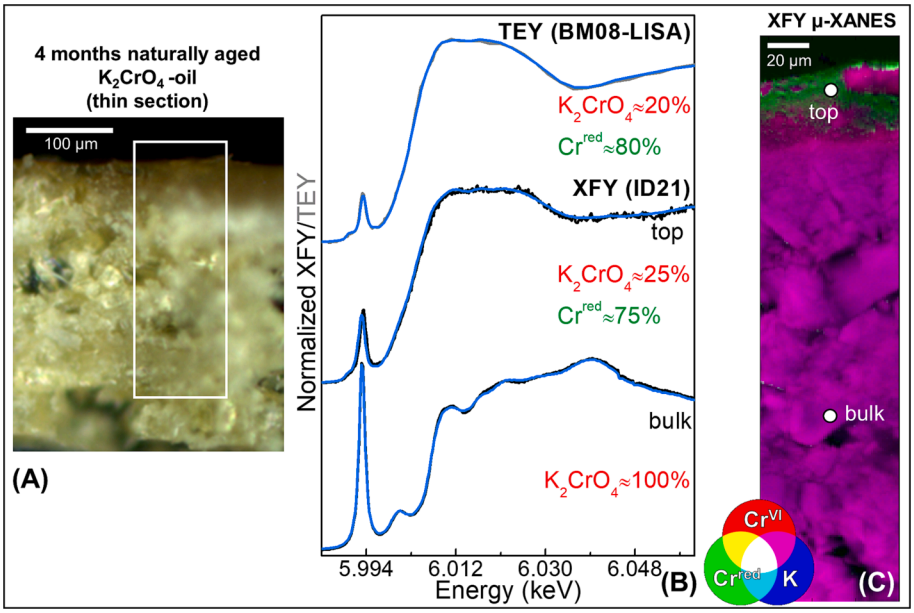

Fig. 4. (A) Microphotograph of a thin section obtained from the 4-months naturally aged K_2CrO_4 paint. (B) Result of the linear combination fit (cyan) of the Cr K-edge XANES spectra of K_2CrO_4, NaCr-$^{V}O_5(C_5H_8O)_2$ and two Cr^{III}-references [namely: Cr $(OH)_3/Cr_2O_3$ and Cr^{III}-acetate/Cr^{III}-acetylacetonate] to the ones collected from the surface of the 4-months naturally aged K_2CrO_4 paint in TEY mode at BM08-LISA (grey) and from the uppermost alteration layer (top) and bulk yellow paint (bulk) of the thin section in XFY mode at ID21 (black). (C) RGB SR μ-XRF images of Cr^{VI}/Cr^{red}/K acquired from the area shown in (A). Spectra of (B) were recorded from the spots illustrated in (C).

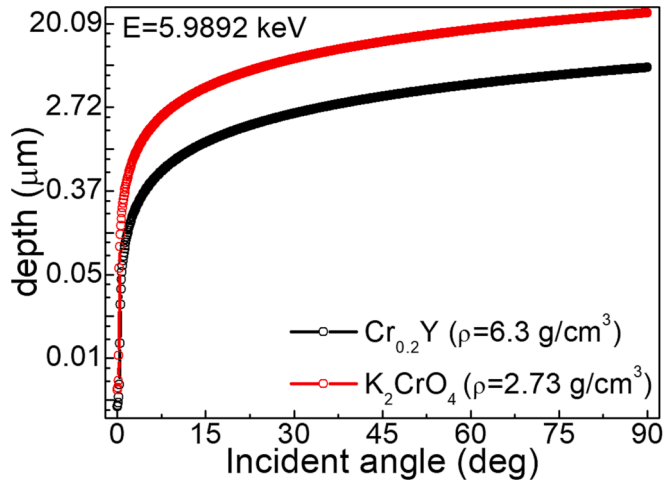

Fig. 5. Plot of the X-ray penetration depth *vs.* incident angle at Cr K-edge energy for $Cr_{0.2}Y$ (black) and K_2CrO_4 (red).

(i) complete loss of stratigraphic information;
(ii) constraints related to the size and surface homogeneity of the analyzed sample, that have to be at least of the order of thousands of μm^2. This implies that some historical paint fragments, often having sizes of the order of only few μm^2 or below, will be not analysable by TEY-XANES with X-ray macro-beams;
(iii) impossibility to measure varnished/coated samples. The presence of a superficial organic layer with thickness greater than 5 μm will completely block the signal of the electrons arising from the paint surface underneath.

In summary, when working with samples of sizes and with a surface homogeneity that are at least of the order of few mm^2, TEY-XANES spectroscopy can be a valuable primary approach to assess the elemental speciation of the paint surface, to determine if the acquisition of high lateral resolution stratigraphic information is relevant or not and, in the case of unvarnished/uncoated samples showing a surface heterogeneity, to make a more accurate selection of the sampling areas from which preparing sections for elemental speciation investigations by μ-XANES spectroscopy in XFY mode.

5. Conclusions

In this paper, we have successfully used Cr K-edge TEY-XANES spectroscopy to selectively probe the composition of the surface of chrome yellow ($PbCr_{0.2}S_{0.8}O_4$) and K_2CrO_4 paints and to quantitatively determine the relative abundances of Cr^{VI} and reduced chromium compounds (i.e., Cr^{III} and Cr^{V}) associated to the alteration process of both classes of chromate compounds. Overall, the study provided accurate qualitative and semi-quantitative information on the newly formed chromium-based phases within the paint matrix, with fully consistent results by comparing the TEY-XANES results recorded directly from the darkened surface of paint fragments with respect to XFY μ-XANES investigations collected from thin sections of the same samples with submicrometric lateral resolution.

Pros and cons of XANES spectroscopy experiments involving the simultaneous combination of XFY and TEY detection were presented and discussed also in relation to μ-XANES analysis in XFY mode, so as to ultimately decrease the efforts spent on sample preparation and minimize the risks of radiation damage. The possibility to perform TEY-XANES spectroscopy using X-ray macro-beams directly at the paint surface has the great advantages of rendering the preparation of samples both faster and easier (i.e., without need of preparing sections) and of reducing the probability of X-ray induced radiation damage, as result of the lower employed fluences. Additionally, the chance to have access to synchrotron beamlines equipped with X-ray macro-beams, where TEY detection systems are already present or can be easily installed, is higher in comparison to those with (sub)micrometer beams.

Nevertheless, it should be noted that, in the context of our research, the TEY-XANES approach using X-ray macro-beams suffers from the following three main limitations: (i) loss of stratigraphic information; (ii) size and surface homogeneity of the analyzed sample that has to be of the order of few mm^2 or below; (iii) possibility to measure only the surface of unvarnished/uncoated paint fragments.

We conclude that, when working with samples that respect such requirements, TEY-XANES spectroscopy can be profitably employed as a primary approach to study the composition of the surface of samples on the submillimetric scale length, thus driving, in a subsequent step, the preparation of sectioned samples and relative measurements at the submicrometer scale length by μ-XANES spectroscopy in XFY mode. Overall, the outcomes of this paper may prompt further research into the application of such combined TEY-XANES/XFY μ-XANES

methodological approach also to the study of the degradation pathways of other pigments (e.g., cadmium reds, orpiment, emerald green…) in fragments from different kinds of unvarnished painted objects (e.g., paintings, sculptures, frescos, papyri, manuscripts, and others) as well as artificially aged paint mock-ups prepared in laboratory.

Declaration of Competing Interest

The authors declare that they have no known competing financial interests or personal relationships that could have appeared to influence the work reported in this paper.

Acknowledgments

The research was financially supported by the Horizon 2020 projects IPERION-CH (H2020-INFRAIA-2014-2015, GA no. 654028) and IPERION-HS (H2020-INFRAIA-2019-1, GA no. 871034) as well as by the Italian project AMIS (Dipartimenti di Eccellenza 2018-2022, funded by MUR and Perugia University). For the beamtime grants received, we thank ESRF for the measurements performed at beamline ID21 (experiments no. HG-64, HG-129 and in-house beamtimes) and the CERIC-ERIC Research Infrastructure (proposal id: 20207042) for those carried out at beamline BM08-LISA of ESRF. LISA is financed by the Consiglio Nazionale delle Ricerche, project N° DFM.AD006.072. FWO (Brussels) projects G054719N and I001919N are also acknowledged for support.

References

[1] L. Samain, G. Silversmit, J. Sanyova, B. Vekemans, H. Salomon, B. Gilbert, F. Grandjean, G.J. Long, R.P. Hermann, L. Vincze, D. Strivay, Fading of modern Prussian blue pigments in linseed oil medium, J. Anal. Atom. Spectrom. 26 (2011) 930–941, https://doi.org/10.1039/C0JA00234H.

[2] L. Samain, F. Grandjean, G.J. Long, P. Martinetto, P. Bordet, J. Sanyova, D. Strivay, Synthesis and fading of eighteenth-century Prussian blue pigments: a combined study by spectroscopic and diffractive techniques using laboratory and synchrotron radiation sources, J. Synchrotron Radiat. 20 (2013) 460–473, https://doi.org/10.1107/S0909049513004585.

[3] M. Radepont, Y. Coquinot, K. Janssens, J.J. Ezrati, W. De Nolf, M. Cotte, Thermodynamic and experimental study of the degradation of the red pigment mercury sulfide, J. Anal. Atom. Spectrom. 30 (2015) 599–612, https://doi.org/10.1039/C4JA00372A, and references therein.

[4] K. Elert, M. Pérez Mendoza, C. Cardell, Direct evidence for metallic mercury causing photo-induced darkening of red cinnabar tempera paints, Commun. Chem. 4 (2021) 1–10, https://doi.org/10.1038/s42004-021-00610-2.

[5] K. Keune, J. Mass, F. Meirer, C. Pottasch, A. van Loon, A. Hull, J. Church, E. Pouyet, M. Cotte, A. Mehta, Tracking the transformation and transport of arsenic sulfide pigments in paints: synchrotron-based X-ray micro-analyses, J. Anal. At. Spectrom. 30 (2015) 813–827, https://doi.org/10.1039/C4JA00424H.

[6] M. Vermeulen, G. Nuyts, J. Sanyova, A. Vila, D. Buti, J.P. Suuronen, K. Janssens, Visualization of As (III) and As (V) distributions in degraded paint micro-samples from Baroque-and Rococo-era paintings, J. Anal. At. Spectrom. 31 (2016) 1913–1921, https://doi.org/10.1039/C6JA00134C.

[7] L. Monico, S. Prati, G. Sciutto, E. Catelli, A. Romani, D.Q. Balbas, Z. Li, S. De Meyer, G. Nuyts, K. Janssens, M. Cotte, J. Garrevoet, G. Falkenberg, V.I. Tardillo Suarez, R. Tucoulou, R. Mazzeo, Development of a multi-method analytical approach based on the combination of synchrotron radiation X-ray micro-analytical techniques and vibrational micro-spectroscopy methods to unveil the causes and mechanism of darkening of “fake-gilded” decorations in a Cimabue painting, J. Anal. At. Spectrom. 37 (2022) 114–129, https://doi.org/10.1039/d1ja00271f.

[8] N. De Keyser, F. Broers, F. Vanmeert, S. De Meyer, F. Gabrieli, E. Hermens, G. Van der Snickt, K. Janssens, K. Keune, Reviving degraded colors of yellow flowers in 17th century still life paintings with macro- and microscale chemical imaging, Sci. Adv. 8 (2022) eabn6344, https://doi.org/10.1126/sciadv.abn6344.

[9] G. Van der Snickt, J. Dik, M. Cotte, K. Janssens, J. Jaroszewicz, W. De Nolf, J. Groenewegen, L. van der Loeff, Characterization of a degraded cadmium yellow (CdS) pigment in an oil painting by means of synchrotron radiation based X-ray techniques, Anal. Chem. 7 (2009) 2600–2610, https://doi.org/10.1021/ac802518z.

[10] G. Van der Snickt, K. Janssens, J. Dik, W. De Nolf, F. Vanmeert, J. Jaroszewicz, M. Cotte, G. Falkenberg, L. van der Loeff, Combined use of synchrotron radiation based micro-X-ray fluorescence, micro-X-ray diffraction, micro-X-ray absorption near-edge, and micro-fourier transform infrared spectroscopies for revealing an alternative degradation pathway of the pigment cadmium yellow in a painting by Van Gogh, Anal. Chem. 84 (2012) 10221–10228, https://doi.org/10.1021/ac3015627.

[11] E. Pouyet, M. Cotte, B. Fayard, M. Salomé, F. Meirer, A. Mehta, E.S. Uffelman, A. Hull, F. Vanmeert, J. Kieffer, M. Burghammer, K. Janssens, F. Sette, J. Mass, 2D X-ray and FTIR micro-analysis of the degradation of cadmium yellow pigment in paintings of Henri Matisse, Appl. Phys. A: Mater. Sci. Process. 121 (2015) 967–980, https://doi.org/10.1007/s00339-015-9239-4, and references therein.

[12] L. Monico, A. Chieli, S. De Meyer, M. Cotte, W. de Nolf, G. Falkenberg, K. Janssens, A. Romani, C. Miliani, Role of the relative humidity and the Cd/Zn stoichiometry in the photooxidation process of cadmium yellows ($CdS/Cd_{1-x}Zn_xS$) in oil paintings, Chem. - Eur. J. 24 (2018) 11584–11593, https://doi.org/10.1002/chem.201801503.

[13] L. Monico, L. Cartechini, F. Rosi, A. Chieli, C. Grazia, S. De Meyer, G. Nuyts, F. Vanmeert, K. Janssens, M. Cotte, W. De Nolf, G. Falkenberg, I.C.A. Sandu, E.S. Tveit, J. Mass, R.P. de Freitas, A. Romani, C. Miliani, Probing the chemistry of CdS paints in The Scream by in situ noninvasive spectroscopies and synchrotron radiation x-ray techniques, Sci. Adv. 6 (2020) eaay3514, doi: 10.1126/sciadv.aay3514.

[14] M. Ghirardello, V. Gonzalez, L. Monico, A. Nevin, D. MacLennan, C. Schmidt Patterson, M. Burghammer, M. Réfrégiers, D. Comelli, M. Cotte, Application of Synchrotron Radiation-Based Micro-Analysis on Cadmium Yellows in Pablo Picasso’s Femme, Microsc. Microanal. 28 (2022) 1504–1513, https://doi.org/10.1017/S1431927622000873.

[15] L. Monico, F. Rosi, R. Vivani, L. Cartechini, K. Janssens, N. Gauquelin, D. Chezganov, J. Verbeeck, M. Cotte, F. d’Acapito, L. Barni, C. Grazia, L. Pensabene Buemi, J.-L. Andral, C. Miliani, A. Romani, Deeper insights into the photoluminescence properties and (photo)chemical reactivity of cadmium red ($CdS_{1-x}Se_x$) paints in renowned twentieth century paintings by state-of-the-art investigations at multiple length scales, Eur. Phys. J. Plus 137 (2022) 311, https://doi.org/10.1140/epjp/s13360-022-02447-7.

[16] F. D’Acapito, X-Ray Absorption Spectroscopy (XAS) Applied to Cultural Heritage, in: S. D’Amico, V. Venuti (Eds.), Handbook of Cultural Heritage Analysis, Springer, Cham, 2022, pp. 45–67, https://doi.org/10.1007/978-3-030-60016-7_4.

[17] K. Janssens, M. Cotte, Using Synchrotron Radiation for Characterization of Cultural Heritage Materials, in: E. Jaeschke, S. Khan, J. Schneider, J. Hastings (Eds.), Synchrotron Light Sources and Free-Electron Lasers, Springer, Cham, 2020, pp. 2457–2483, https://doi.org/10.1007/978-3-030-23201-6_78.

[18] E. Pouyet, B. Fayard, M. Salomé, Y. Taniguchi, F. Sette, M. Cotte, Thin-sections of painting fragments: opportunities for combined synchrotron-based micro-spectroscopic techniques, Heritage Sci. 3 (2015) 1–16, https://doi.org/10.1186/s40494-014-0030-1.

[19] N. Isomura, K. Oh-Ishi, N. Takahashi, S. Kosaka, A practical method for determining film thickness using X-ray absorption spectroscopy in total electron yield mode, J. Synchrotron Rad. 28 (2021) 1820–1824, https://doi.org/10.1107/S1600577521009401.

[20] A. Erbil, G.S. Cargill III, R. Frahm, R.F. Boehme, Total-electron-yield current measurements for near-surface extended x-ray-absorption fine structure, Phys. Rev. B 37 (1988) 2450–2464, https://doi.org/10.1103/PhysRevB.37.2450.

[21] W.T. Elam, J.P. Kirkland, R.A. Neiser, P.D. Wolf, Depth dependence for extended x-ray-absorption fine-structure spectroscopy detected via electron yield in He and in vacuum, Phys. Rev. B 38 (1988) 26–30, https://doi.org/10.1103/PhysRevB.38.26.

[22] G. Ciatto, F. d’Acapito, S. Sanna, V. Fiorentini, A. Polimeni, M. Capizzi, S. Mobilio, F. Boscherini, Comparison between experimental and theoretical determination of the local structure of the $GaAs_{1-y}N_y$ dilute nitride alloy, Phys. Rev. B 71 (2005), 115210, https://doi.org/10.1103/PhysRevB.71.115210.

[23] S. Padovani, I. Borgia, B. Brunetti, A. Sgamellotti, A. Giulivi, F. D’Acapito, P. Mazzoldi, C. Sada, G. Battaglin, Silver and copper nanoclusters in the lustre decoration of Italian Renaissance pottery: an EXAFS study, Appl. Phys. A Mater. Sci. Process. 79 (2004) 229–233, https://doi.org/10.1007/s00339-004-2516-2.

[24] X. Mi, T. Li, J. Wang, Y. Hu, Evaluation of Salt-Induced Damage to Aged Wood of Historical Wooden Buildings, Int. J. Anal. Chem. 2020 (2020) 887371, https://doi.org/10.1155/2020/8873713.

[25] L. Zanella, F. Casadio, K.A. Gray, R. Warta, Q. Ma, J.F. Gaillard, The darkening of zinc yellow: XANES speciation of chromium in artist’s paints after light and chemical exposures, J. Anal. At. Spectrom. 26 (2011) 1090–1097, https://doi.org/10.1039/C0JA00151A.

[26] L. Cartechini, C. Miliani, B.G. Brunetti, A. Sgamellotti, C. Altavilla, E. Ciliberto, F. D’acapito, X-ray absorption investigations of copper resinate blackening in a XV century Italian painting, Appl. Phys. A Mater. Sci. Process 92 (2008) 243–250, https://doi.org/10.1007/s00339-008-4498-y.

[27] L. Monico, L. Sorace, M. Cotte, W. De Nolf, K. Janssens, A. Romani, C. Miliani, Disclosing the Binding Medium Effects and the Pigment Solubility in the (Photo) reduction Process of Chrome Yellows ($PbCrO_4/PbCr_{1-x}S_xO_4$), ACS Omega 4 (2019) 6607–6619, https://doi.org/10.1021/acsomega.8b03669.

[28] L. Monico, K. Janssens, M. Cotte, L. Sorace, F. Vanmeert, B.G. Brunetti, C. Miliani, Chromium speciation methods and infrared spectroscopy for studying the chemical reactivity of lead chromate-based pigments in oil medium, Microchem. J. 124 (2016) 272–282, https://doi.org/10.1016/j.microc.2015.08.028.

[29] L. Monico, K. Janssens, M. Cotte, A. Romani, L. Sorace, C. Grazia, B.G. Brunetti, C. Miliani, Synchrotron-based X-ray spectromicroscopy and electron paramagnetic resonance spectroscopy to investigate the redox properties of lead chromate pigments under the effect of visible light, J. Anal. At. Spectrom. 30 (2015) 1500–1510, https://doi.org/10.1039/C5JA00091B.

[30] L. Monico, K. Janssens, E. Hendriks, F. Vanmeert, G. Van der Snickt, M. Cotte, G. Falkenberg, B.G. Brunetti, C. Miliani, Evidence for Degradation of the Chrome Yellows in Van Gogh’s Sunflowers: A Study Using Noninvasive In Situ Methods and Synchrotron-Radiation-Based X-ray Techniques, Angew. Chem., Int. Ed. Engl. 54 (2015) 13923–13927, https://doi.org/10.1002/anie.201505840.

[31] L. Monico, G. Van der Snickt, K. Janssens, W. De Nolf, C. Miliani, J. Dik, M. Radepont, E. Hendriks, M. Geldof, M. Cotte, Degradation Process of Lead Chromate in Paintings by Vincent van Gogh Studied by Means of Synchrotron X-ray Spectromicroscopy and Related Methods. 2. Original Paint Layer Samples, Anal. Chem. 83 (2011) 1224–1231, https://doi.org/10.1021/ac1025122.
[32] L. Monico, M. Cotte, F. Vanmeert, L. Amidani, K. Janssens, G. Nuyts, J. Garrevoet, G. Falkenberg, P. Glatzel, A. Romani, C. Miliani, Damages Induced by Synchrotron Radiation-Based X-ray Microanalysis in Chrome Yellow Paints and Related Cr-Compounds: Assessment, Quantification, and Mitigation Strategies, Anal. Chem. 92 (2020) 14164–14173, https://doi.org/10.1021/acs.analchem.0c03251.
[33] L. Bertrand, S. Schöeder, D. Anglos, M.B. Breese, K. Janssens, M. Moini, A. Simon, Mitigation strategies for radiation damage in the analysis of ancient materials, *TrAC*, Trends Anal. Chem. 66 (2015) 128–145, https://doi.org/10.1016/j.trac.2014.10.005.
[34] L. Monico, K. Janssens, C. Miliani, B.G. Brunetti, M. Vagnini, F. Vanmeert, G. Falkenberg, A. Abakumov, Y. Lu, H. Tian, J. Verbeeck, M. Radepont, M. Cotte, E. Hendriks, M. Geldof, L. van der Loeff, J. Salvant, M. Menu, Degradation Process of Lead Chromate in Paintings by Vincent van Gogh Studied by Means of Spectromicroscopic Methods. 3. Synthesis, Characterization, and Detection of Different Crystal Forms of the Chrome Yellow Pigment, Anal. Chem. 85 (2013) 851–859, https://doi.org/10.1021/ac302158b.
[35] L. Monico, K. Janssens, E. Hendriks, B.G. Brunetti, C. Miliani, Raman study of different crystalline forms of $PbCrO_4$ and $PbCr_{1-x}S_xO_4$ solid solutions for the noninvasive identification of chrome yellows in paintings: a focus on works by Vincent van Gogh, J. Raman Spectrosc. 45 (2014) 1034–1045, https://doi.org/10.1002/jrs.4548.
[36] F. D'Acapito, G.O. Lepore, A. Puri, A. Laloni, F. La Manna, E. Dettona, A. De Luisa, A. Martin, The LISA beamline at ESRF, J. Synchrotron Radiat. 26 (2019) 551–558, https://doi.org/10.1107/S160057751801843X.
[37] P. Raimondi, ESRF-EBS: The Extremely Brilliant Source Project, Synchrotron Radiation News 29 (2016) 8–15, https://doi.org/10.1080/08940886.2016.1244462.
[38] M. Cotte, E. Pouyet, M. Salome, C. Rivard, W. De Nolf, H. Castillo-Michel, T. Fabris, L. Monico, K. Janssens, T. Wang, P. Sciau, L. Verger, L. Cormier, O. Dargaud, E. Brun, D. Bugnazet, B. Fayard, B. Hesse, A. Pradas del Real, G. Veronesi, J. Langlois, N. Balcar, Y. Vandenberghe, V.A. Sole, J. Kieffer, R. Barrett, C. Cohen, C. Cornu, R. Baker, E. Gagliardini, E. Papillon, J. Susini, The ID21 X-ray and infrared microscopy beamline at the ESRF: status and recent applications to artistic materials, J. Anal. Atom. Spectrom. 32 (2017) 477–493, https://doi.org/10.1039/C6JA00356G.
[39] F. d'Acapito (Ed.), Activity Report at the Italian CRG Beamline at ESRF, 2018, p. n.6, https://doi.org/10.5281/zenodo.7379990.
[40] G. Tourillon, E. Dartyge, A. Fontaine, M. Lemonnier, F. Bartol, Electron yield X-ray absorption spectroscopy at atmospheric pressure, Phys. Lett. A 121 (1987) 251–257, https://doi.org/10.1016/0375-9601(87)90015-6.
[41] T. Ishikawa, K. Tamasaku, M. Yabashi, High-resolution X-ray monochromators, Nucl. Instrum., Methods Phys. Res., Sect. A 547 (2005) 42–49, https://doi.org/10.1016/j.nima.2005.05.010.
[42] M. Cotte, T. Fabris, G. Agostini, D. Motta Meira, L. De Viguerie, V.A. Solé, Watching kinetic studies as chemical maps using open-source software, Anal. Chem. 88 (2016) 6154–6160, https://doi.org/10.1021/acs.analchem.5b04819.
[43] L. Monico, G. Van der Snickt, K. Janssens, W. De Nolf, C. Miliani, J. Verbeeck, H. Tian, H. Tan, J. Dik, M. Radepont, M. Cotte, Degradation process of lead chromate in paintings by Vincent van Gogh studied by means of synchrotron X-ray spectromicroscopy and related methods. 1. Artificially aged model samples, Anal. Chem. 83 (2011) 1214–1223, https://doi.org/10.1021/ac102424h.
[44] B. Ravel, M. Newville, ATHENA, ARTEMIS, HEPHAESTUS: data analysis for X-ray absorption spectroscopy using IFEFFIT, J. Synchrotron Radiat. 12 (2005) 537–541, https://doi.org/10.1107/S0909049505012719.
[45] A.J. Achkar, T.Z. Regier, H. Wadati, Y.J. Kim, H. Zhang, D.G. Hawthorn, Bulk sensitive x-ray absorption spectroscopy free of self-absorption effects, Phys. Rev. B 83 (2011) 081106(R), https://doi.org/10.1103/PhysRevB.83.081106.
[46] D. Ingerle, G. Pepponi, F. Meirer, P. Wobrauschek, C. Streli, JGIXA — A software package for the calculation and fitting of grazing incidence X-ray fluorescence and X-ray reflectivity data for the characterization of nanometer-layers and ultra-shallow-implants, Spectrochim. Acta Part B At. Spectrosc. 118 (2016) 20–28, https://doi.org/10.1016/j.sab.2016.02.010.
[47] A. Nemethy, L. Kover, I. Cserny, D. Varga, P.B. Barna, The KLL and KLM Auger spectra of 3d transition metals, Z= 23–26, J. Electron Spectrosc. Relat. Phenom. 82 (1996) 31–40, https://doi.org/10.1016/S0368-2048(96)03038-1.
[48] A. Pantelouris, H. Modrow, M. Pantelouris, J. Hormes, D. Reinen, The influence of coordination geometry and valency on the K-edge absorption near edge spectra of selected chromium compounds, Chem. Phys. 300 (2004) 13–22, https://doi.org/10.1016/j.chemphys.2003.12.017.
[49] M. Tromp, J. Moulin, G. Reid, J. Evans, Cr K-Edge XANES Spectroscopy: Ligand and Oxidation State Dependence—What is Oxidation State? AIP Conf. Proc. 882 (2007) 699–701, https://doi.org/10.1063/1.2644637.
[50] M.L. Peterson, G.E. Brown, G.A. Parks, C.L. Stein, Differential redox and sorption of Cr (III/VI) on natural silicate and oxide minerals: EXAFS and XANES results, Geochim. Cosmochim. Acta 61 (1997) 3399–3412, https://doi.org/10.1016/S0016-7037(97)00165-8.
[51] F. Farges, Chromium speciation in oxide-type compounds: application to minerals, gems, aqueous solutions and silicate glasses, Phys. Chem. Miner. 36 (2009) 463–481, https://doi.org/10.1007/s00269-009-0293-3.
[52] S.L. Schroeder, G.D. Moggridge, T. Rayment, R.M. Lambert, In situ probing of the near-surface properties of heterogeneous catalysts under reaction conditions: An introduction to total electron-yield XAS, J. Mol. Catal. A: Chem. 119 (1997) 357–365, https://doi.org/10.1016/S1381-1169(96)00499-2.
[53] A. Krol, C.S. Lin, Z.H. Ming, C.J. Sher, Y.H. Kao, C.T. Chen, F. Sette, Y. Ma, G. C. Smith, Y.Z. Zhu, D.T. Shaw, X-ray-absorption studies of Y-Ba-Cu-O and Bi-Sr-Ca-Cu-O films at oxygen K edge by means of fluorescence and total electron yield: A comparison of two techniques, Phys. Rev. B 42 (1990) 2635–2638, https://doi.org/10.1103/PhysRevB.42.2635.
[54] S. Padovani, F. D'Acapito, C. Sada, E. Cattaruzza, F. Gonella, N. Argiolas, M. Bazzan, C. Maurizio, P. Mazzoldi, Er^{3+}–Li^{+} ion exchange in lithium niobate crystals: an EXAFS study, Eur. Phys. J. B 32 (2003) 157–161, https://doi.org/10.1140/epjb/e2003-00084-8.